The Effect of Heat Transfer and Slip Condition on Peristaltic Transport of MHD non-Newtonian Fluid Across Tapered porous Channel

Asia Amer[1] and Mohammed Ali Murad[2]

[1]Department of Mathematics – College of Science – University of Diyala, Diyala, Iraq.
[2]Department of Mathematics – College of Basic Education – University of Diyala, Diyala, Iraq.

[1] asiaamir8585@gmail.com

Abstract

In this paper, the effect of heat transfer and slip conditions on peristaltic transport of Magneto hydrodynamics (MHD) non-Newtonian fluid across tapered porous channel are studied. The mathematical equations for Bingham fluid model are developed and use the perturbation method to obtain the analytic solutions of the expressions for axial velocity and temperature distribution under the assumption of long wavelength and low Reynolds numbers. The effects of all parameters that appear in the problem are analyzed through graphs. The results showed that axial velocity increased by increasing Q and the opposite for rising m. Also, the temperature profile increases by increasing k, ϕ_1 and ϕ_2 with the opposite behavior for φ and M. MATHEMATICA software is used for computational results and plotting all figures.

Keywords: Peristaltic transport, Slip condition, Magnetic Field, Bingham Fluid.

تأثير انتقال الحرارة وشرط الانزلاق على الانتقال التمعجي لمائع لانيوتيني مكنتوهييدرو داينمك عبر قناة مسامية مدببة

اسيا عامر سعيد ومحمد علي مراد

قسم الرياضيات –كلية العلوم- جامعة ديالى
قسم الرياضيات-كلية التربية الاساسية-جامعة ديالى

الخلاصة

في هذا البحث تمت دراسة تأثير انتقال الحرارة وشرط الانزلاق على الانتقال التمعجي للمائع لا نيوتيني مكنتو هيدرو داينمكي عبر قناة مسامية مدببة. تم تطوير المعادلات الرياضية لنموذج مائع بينغهام واستخدام طريقة الاضطراب للحصول على الحلول التقريبية للتعبير عن السرعة المحورية وتوزيع درجة الحرارة على افتراض الطول الموجي الطويل وعدد رينولدز المنخفض. تم تحليل تأثيرات جميع المعلمات التي تظهر في المسالة من خلال الرسوم البيانية. أظهرت النتائج أن السرعة المحورية تزداد بزيادة Q والعكس مع زيادة m. أيضًا ، بيان تعريف درجة الحرارة بزيادة ϕ_1, ϕ_2 و k مع السلوك المعاكس لـ φ و. يتم استخدام برنامج MATHEMATICA للنتائج الحسابية ورسم جميع الأشكال.

الكلمات المفتاحية: النقل التمعجي، حالة الانزلاق، المجال المغناطيسي، سائل بينغهام

Introduction

Peristaltic flow is simply a form of fluid transport inside a channel or tube induced by the progressive wave of area contraction or expansion along the axial axis direction of a flexible walls. Peristaltic flow has recently attracted a lot of attention due to its implications in industry and physiology. The human body experiences peristalsis flow in the movement of chime through the digestive system, urine via the ureter, and swallowed food through the esophagus as well as numerous others the non-Newtonian fluids deviate from the classical Newtonian linear relationship between the shear stress and shear rate, for example honey, blood and processing of food are considered non-Newtonian fluid. Due to complex rheological properties, it is difficult to suggest a single model which exhibits all properties of non-Newtonian fluids. Machines have been designed on the principle of peristaltic. In recent years, the effects of heat transfer on peristaltic transport of non-Newtonian fluid in the present of magnetic field receive considerable attentions due to its application in biomedical sciences. It is now a well-accepted

fact that the peristaltic flows of magneto hydrodynamic (MHD) fluids are important in medical sciences and bioengineering. The MHD characteristics are useful in the development of magnetic devices, cancer tumor treatment, hyperthermia and blood reduction during surgery. Flows through porous medium occur in filtration of fluids and seepage of water in river beds [1,2].

This type of flow is highly useful in the design of a variety of biomedical devices, such as the heat-lung device that keeps blood flowing during risky surgeries [3]. This subject was first investigated by Shapiro et al. and Lew et al. [4,5]. The concept of peristaltic transport has been subjected to a number of hypotheses, the most well-known of which are the long wavelength and low Reynolds number. The viscosity of a non- Newtonian fluid varies depending on the applied tension or force. It's a fluid whose flow characteristics aren't characterized by a single constant viscosity value. When the peristaltic pump is activated, physiological fluid with constant viscosity fail to provide an accurate hold. The lymphatic vessels, tiny blood vessels, and the intestines are all involved in the transmission. The majority of peristalsis research was used on a viscosity that was consistent. Several recent research [6-9] looked in to the impact of changing viscosity when the viscosity is only based on distance. However, other studies looked at the effect of viscosity when it is temperature dependent [10-12]. It has also been discovered that heat and mass transfer play important roles in peristaltic flow, such as in blood flux processes, kidney dialysis, and cancer medication. Bifurcation analysis for a two-dimensional peristaltic driven flow of power–law fluid in asymmetric channel [13]. MHD effect on peristaltic transport for rabinowitsch fluid through a porous medium in cilia channel [14]. Impacts of heat and mass transfer on magneto hydrodynamic peristaltic flow having temperature dependent properties in an inclined channel [15]. The present study addresses the effect of heat transfer and slip conditions on peristaltic transport of MHD non-Newtonian fluid across tapered porous channel. The differential equations of the fluid flow were resolved subject to related boundary conditions (slip conditions). The non-Newtonian Bingham fluid was considered in this study. Open form solutions for this problem are obtained via perturbation method. The results are illustrated by plotted graphical results for axial velocity and temperature distraction.

**Formulation in Mathematics**

Consider a peristaltic transport of an incompressible MHD non‑Newtonian fluid with variable viscosity in a two-dimensional non-uniform tapered porous channel of width $(a_1 + a_2)$. Figure1 gives the schematic diagram of the non-uniform tapered channel. The flow is created by waves propagating down the channel walls at a constant speed of c, with varying wave amplitudes, phase angles, and channel widths. In the stationary frame of reference $(\bar{X}, \bar{Y})$, let $\bar{H}_1$ and $\bar{H}_2$ represent the right and the left side wall respectively. To investigate the impact of a uniform magnetic field on fluid flow, it is applied in the Y-direction with absence of an electric field. Convective conditions were used to study heat transfer. The deformable walls are given by [16,17]

$$\bar{Y} = \bar{H}_1(\bar{X}, \bar{t}) = a_1 + \bar{b}\bar{X} + \bar{\phi}_1 \cos\left(\frac{2\pi}{\lambda}(\bar{X} - c\bar{t})\right) \quad\text{...(1)}$$

for the right-hand side wall,

$$\bar{Y} = \bar{H}_2(\bar{X}, \bar{t}) = -a_2 - \bar{b}\bar{X} - \bar{\phi}_2 \cos\left(\frac{2\pi}{\lambda}(\bar{X} - c\bar{t}) + \bar{\varphi}\right) \quad\text{...(2)}$$

for the left hand side wall, where λ is the wavelength, $\bar{\phi}_1$ and $\bar{\phi}_2$ are the amplitudes of the waves, $\bar{t}$ is the time, $\bar{\varphi}$ is the phase difference which varies in the range $0 \leq \bar{\varphi} \leq \pi$. Further $a_1, a_2, \bar{\phi}_1, \bar{\phi}_2$ and $\bar{\varphi}$ satisfy $\bar{\phi}_1^2 + \bar{\phi}_2^2 + 2\bar{\phi}_1\bar{\phi}_1 \cos \bar{\varphi} \leq (a_1 + a_2)^2$ so that the boundaries that do not cross each other.
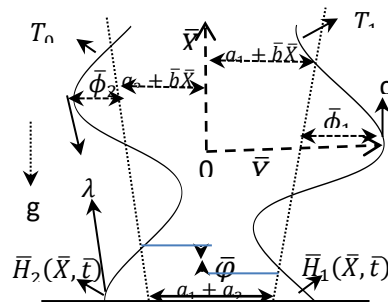
Figure 1: The figure represents an asymmetric channel.[18]

Basic and Constitutive equations

The main governing equation that characterize the flow in the current problem are given by [19,20]

$$\frac{\partial \bar{U}}{\partial \bar{X}} + \frac{\partial \bar{V}}{\partial \bar{Y}} = 0, \dots\dots\dots(3)$$

$$\rho \left(\frac{\partial \bar{U}}{\partial \bar{t}} + \bar{U}\frac{\partial \bar{U}}{\partial \bar{X}} + \bar{V}\frac{\partial \bar{U}}{\partial \bar{Y}} \right) = -\frac{\partial \bar{P}}{\partial \bar{X}} + \frac{\partial \bar{\tau}_{\bar{X}\bar{X}}}{\partial \bar{X}} + \frac{\partial \bar{\tau}_{\bar{X}\bar{Y}}}{\partial \bar{Y}} + \rho g \bar{\alpha}(\bar{T} - T_0) - \sigma' B_0^2 \bar{U} - \frac{\bar{\eta}(y)}{\bar{k}}\bar{U}, \dots\dots(4)$$

$$\rho \left(\frac{\partial \bar{V}}{\partial \bar{t}} + \bar{U}\frac{\partial \bar{V}}{\partial \bar{X}} + \bar{V}\frac{\partial \bar{V}}{\partial \bar{Y}} \right) = -\frac{\partial \bar{P}}{\partial \bar{Y}} + \frac{\partial \bar{\tau}_{\bar{Y}\bar{X}}}{\partial \bar{X}} + \frac{\partial \bar{\tau}_{\bar{Y}\bar{Y}}}{\partial \bar{Y}} - \frac{\bar{\eta}(y)}{\bar{k}}\bar{V}, \dots\dots(5)$$

$$\rho C_p \left(\frac{\partial \bar{T}}{\partial \bar{t}} + \bar{U}\frac{\partial \bar{T}}{\partial \bar{X}} + \bar{V}\frac{\partial \bar{T}}{\partial \bar{Y}} \right) = \kappa \left(\frac{\partial^2 \bar{T}}{\partial \bar{X}^2} + \frac{\partial^2 \bar{T}}{\partial \bar{Y}^2} \right) + \bar{\tau}_{\bar{X}\bar{X}}\frac{\partial \bar{U}}{\partial \bar{X}} + \bar{\tau}_{\bar{X}\bar{Y}}\frac{\partial \bar{V}}{\partial \bar{X}} + \bar{\tau}_{\bar{Y}\bar{X}}\frac{\partial \bar{U}}{\partial \bar{Y}} + \bar{\tau}_{\bar{Y}\bar{Y}}\frac{\partial \bar{V}}{\partial \bar{Y}}, \dots(6)$$

The associated dimensional form boundary condition [1,5] are

$$\left. \begin{array}{l} \bar{U} + \bar{\beta}\frac{\partial \bar{U}}{\partial \bar{Y}} = 0, \bar{T} = T_1 \quad at \; \bar{Y} = \bar{H}_1 \\ \bar{U} - \bar{\beta}\frac{\partial \bar{U}}{\partial \bar{Y}} = 0 \;\;, \;\; \bar{T} = T_0 \quad at \; \bar{Y} = \bar{H}_2 \end{array} \right\} \dots\dots(7)$$

Where g, $\bar{\eta}(y)$, $\bar{k}$, T, κ , $\bar{\beta}$ and C_p are represent gravity acceleration, variable viscosity, permeability, temperature, thermal conductinty, velocity-slip parameter and specific heat respectively. The magnetic part is added to the momentum equation by using Lorentz force in absent of electric field (for more detail [21]).

The non-Newtonian Bingham plastic fluid is chosen and the extra stresses are defined by given tensor [16] as follows

$$\bar{\tau} = 2\bar{\eta}(y)D + 2\tau_0 \tilde{D}, \dots\dots(8)$$

where the deformation tensor D and the tensor $\tilde{D}$ are given by

$$D = \frac{1}{2}\left(\nabla \vec{V} + \left(\nabla \vec{V} \right)^T \right), \quad \tilde{D} = \frac{D}{\sqrt{2traD^2}} \dots\dots(9)$$

The relate between fixed and move frames are introduced as

$$\left.\begin{array}{l} \bar{x} = \bar{X} - c\bar{t}, \quad \bar{y} = \bar{Y} \ , \ \bar{u}(\bar{x},\bar{y}) = \bar{U}(\bar{X},\bar{Y},\bar{t}) - c \ , \\ \bar{v}(\bar{x},\bar{y}) = \bar{V}(\bar{X},\bar{Y},\bar{t}), \bar{p}(\bar{x},\bar{y}) = \bar{P}(\bar{X},\bar{Y},\bar{t}), T(\bar{x},\bar{y}) = \bar{T}(\bar{X},\bar{Y},\bar{t}). \end{array}\right\} \quad \text{...............(10)}$$

and the dimensionless variables are

$$\left.\begin{array}{l} \bar{x} = \lambda x \ , \bar{y} = a_1 y \ , \bar{u} = cu \ , \bar{v} = cv \ , \bar{t} = \frac{\lambda}{c} t \ , \ \bar{p} = \frac{c\eta_0 \lambda}{a_1^2} p, \\[4pt] Re = \frac{\rho a_1 c}{\eta_0} \ , \bar{\phi}_1 = a_1 \phi_1 \ , \delta = \frac{a_1}{\lambda} \ , \bar{H} = a_1 H, Q^* = a_1 c\Theta \ , \\[4pt] \bar{\phi}_2 = a_1 \phi_2 \ , \bar{\beta} = a_1 \beta, \bar{q} = a_1 cF \ , \bar{k} = a_1^2 k \ , \bar{\tau}_{ij} = \frac{c \eta_0}{a_1} \tau_{ij}, \\[4pt] \bar{b} = a_1 b, \ \theta = \frac{T - T_0}{T_1 - T_0}, Pr = \frac{C_p \eta_0}{\kappa}, Ec = \frac{c^2}{C_p(T_1 - T_0)}, \\[4pt] \bar{\psi} = ca_1 \psi \ , \ A^2 = M^2 + \frac{1}{k}, \eta(y) = \frac{\bar{\eta}(y)}{\eta_0}, \\[4pt] Bn = \frac{a_1 \tau_0}{c \eta_0} \ , M^2 = \frac{\sigma' B_0^2 a_1^2}{\eta_0}, Gr = \frac{\rho g \bar{\alpha} \, a_1^2 (T_1 - T_0)}{c \eta_0}. \end{array}\right\} \quad \text{............ (11)}$$

Equations (10) and (11) are used in equations (1)-(9) and then applying $Re \ll 1$, $\delta \ll 1$ and the relations $u = \psi_y$ and $v = -\delta \psi_x$ to obtain the following dimensionless governing equations

$$y = H_1(x) = 1 + bx + \phi_1 \cos(2\pi x) \ , \text{..(12)}$$

$$y = H_2(x) = -a - bx - \phi_2 \cos(2\pi x + \bar{\varphi}) \ , \ a = \frac{a_2}{a_1} , \text{................................(13)}$$

$$\frac{\partial p}{\partial x} = \frac{\partial}{\partial y} \tau_{xy} + Gr\theta - M^2(\psi_y + 1) - \frac{\eta(y)}{k}(\psi_y + 1), \text{...............................(14)}$$

$$\frac{\partial p}{\partial y} = 0, \text{...(15)}$$

$$\frac{\partial^2 \theta}{\partial y^2} = -Br\tau_{xy}\psi_{yy} \ , \quad Br = PrEc \text{...(16)}$$

$$\left.\begin{array}{ll} \psi_y + \beta\psi_{yy} = -1 \ , \theta = 1 & at \ y = H_1 \\ \psi_y - \beta\psi_{yy} = -1, \ \theta = 0 & at \ y = H_2 \end{array}\right\} \text{.........................(17)}$$

$$\tau_{xx} = \tau_{yy} = 0, \ \tau_{xy} = \eta(y)\psi_{yy} + B_n, \text{...(18)}$$

Where, $Br = EcPr$, is the Brinkman number. The Reynolds model of viscosity is used to describe the variable viscosity. let as consider

$$\eta(y) = e^{-\alpha y} \dots\dots\dots\dots\dots\dots\dots\dots\dots\dots\dots\dots\dots\dots\dots\dots\dots\dots\dots\dots\dots\dots\dots(19)$$

Where α is the Reynolds model parameter which is constant. Using the maclaurian series expansion, neglecting squares and higher powers of α, equation (19) can be written as

$$\eta(\alpha) = 1 - \alpha y, \quad \alpha \ll 1$$

Compensating equation (19) and (18) in to equation (14) in light of equation (15) and driving the result with respect y provides

The dimensionless volume flow rate F in the wave frame defined by

$$F = \int_{H_2(x)}^{H_1(x)} \frac{\partial \psi}{\partial y} dy = \psi(H_1(x)) - \psi(H_2(x)), \dots\dots\dots\dots\dots\dots\dots\dots\dots\dots(20)$$

or one can write

$\psi = \frac{F}{2}$ at the right wall and $\psi = -\frac{F}{2}$ at the left wall of the channel. and $\Theta = F + 2 - 2m$ where Θ is the time mean flow rate.

The equation (15) and equation (18) are used into equation (14) and deriving the conclusion with respect to y produces,

$$\psi_{yyyy} - \alpha y \psi_{yyyy} - 2\alpha\psi_{yyy} + Gr\theta_y - A^2\psi_{yy} + \frac{\alpha y}{k}\psi_{yy} + \frac{\alpha}{k}\psi_y + \frac{\alpha}{k} = 0 \dots\dots\dots\dots\dots(21)$$

From equation (16) and (18) having

$$\theta yy = -Br\left[\psi_{yy}^2 - \alpha y\psi_{yy}^2 + Bn\psi_{yy}\right] \dots\dots\dots\dots\dots\dots\dots\dots\dots\dots\dots\dots(22)$$

Solution of the Problem

The system of nonlinear partial differential equations, ((21) and (22)) in the aforementioned equations that are difficult to solve precisely. As a result, to solve it, using an approximated

approach through the perturbation method. For small values of viscosity ($\alpha \ll 1$) and Grashof number ($Gr \ll 1$), stream function and temperature expand as follows

$$\left.\begin{array}{l} \psi = \sum_{i=0}^{\infty}(\alpha)^i \psi_i + O(\alpha^2) \\ \theta = \sum_{i=0}^{\infty}(Gr)^i \theta_i + O(Gr^2) \end{array}\right\} \quad \text{............(23)}$$

The zeroth and first order systems are obtained by using equation (23) into equations (21) and (22) with the relevant boundary conditions (equations (17) and (20)) and then collection the coefficients of like power of α and Gr.

4.1 Zeroth Order System

$$\psi_{0yyyy} - A^2\psi_{0yy} = 0, \quad \text{...........................(24)}$$

$$\theta_{0yy} + Br\psi_{0yy}^2 + BrBn\psi_{0yy} = 0, \quad \text{..............(25)}$$

with the boundary constraints that go along with it

$$\left.\begin{array}{llll} \psi_0 = \frac{F}{2}, & \psi_{0y} + \beta\psi_{0yy} = -1, & \theta_0 = 1 & at\ y = H_1 \\ \psi_0 = -\frac{F}{2}, & \psi_{0y} - \beta\psi_{0yy} = -1, & \theta_0 = 0 & at\ y = H_2 \end{array}\right\} \quad \text{.........(26)}$$

4.2 First Order System

$$\psi_{1yyyy} - y\psi_{0yyyy} - 2\psi_{0yyy} + \theta_{oy} - A^2\psi_{1yy} + \frac{y}{k}\psi_{0yy} + \frac{1}{k}(\psi_{0y} + 1) = 0 \quad \text{.............(27)}$$

$$\theta_{1yy} + 2Br\psi_{0yy}\psi_{1yy} - yBr\psi_{0yy}^2 + BrBn\psi_{1yy} = 0, \quad \text{...........(28)}$$

with the corresponding boundary conditions

$$\left.\begin{array}{llll} \psi_1 = 0, & \psi_{1y} + \beta\psi_{1yy} = 0, & \theta_1 = 0, & at\ y = H_1 \\ \psi_1 = 0, & \psi_{1y} - \beta\psi_{1yy} = 0, & \theta_1 = 0, & at\ y = H_2 \end{array}\right\} \quad \text{.............(29)}$$

All calculations are performed using the MATHEMATICA software, and the zeroth system's solution with the required boundary conditions is carried out.

$$\psi_0 = \frac{\frac{e^{Ay}c_1}{A} + \frac{e^{-Ay}c_2}{A}}{A} + c_3 + yc_4;$$

$$\theta_0 = -\frac{Br(c_2^2 e^{-2Ay} + 4Bnc_2 e^{-Ay} + 4Bnc_1 e^{Ay} + c_1^2 e^{2Ay} + 4A^2 c_1 c_2 y^2)}{4A^2} + c_5 + yc_6;$$

where c_i, $i = 1,2,\dots,6$ are constants discovered by the use of boundary conditions. The zeroth order solution is used to solve the first order system with the relevant boundary conditions which is.

$$\psi_1 = \frac{1}{24A^5 k} e^{-2Ay} \Big(-Brc_2^2 k + Brc_1^2 e^{4Ay} k$$
$$+ 3c_1 e^{3Ay}\big(-7 - 10BnBrk - 2A^3 ky + 2A(3 + 2BnBrk)y + 2A^4 ky^2$$
$$- A^2(3k + 2y^2)\big)$$
$$- c_2 e^{Ay}\big(-3(7 + 10BnBrk) - 6A(3 + 2BnBrk)y + 6A^4 ky^2 - 3A^2(3k + 2y^2)$$
$$+ 2A^3 ky(3 + 4Brc_1 e^{Ay}y^2)\big)$$
$$+ 12A^3 e^{Ay}(e^{Ay}(1 + c_4 + c_6 k)y^2 + 2e^{2Ay}c_9 + 2k*c_{10})\Big) + c_{11} + y*c_{12};$$

$$\theta_1 = Br\Big(-\frac{c_2^2 e^{-2Ay}(-\frac{1}{A}-y)}{4A^2} + \frac{1}{3}c_1 c_2 y^3 + \frac{c_1^2 e^{2Ay}(-\frac{1}{A}+y)}{4A^2}\Big) + c_{13} + yc_{14};$$

also $i = 9,10,\dots,16$ are constants discovered through the application of boundary conditions.

Results and Discussion

The approximate solution via perturbation method is calculated for velocity and temperature profile. Further, this section displays the computational results with help of graphs as shown in figs.2 -23.

Velocity Distribution u

The behavior of the parameters involved in the simulation is depicted graphically. u represents velocity on the axis of flow. The effects of various values of $M, k, \alpha, \beta, \phi_1, \phi_2, m, \varphi, Br, Bn,$ and Q on the axial velocity u are depicted in Figs. 2 - 12. As seen in the figures, the velocity distribution has a parabolic behavior. Figs.2 and 3 demonstrates M and β influence on u. It is observed that when M and β is rise, the axis multiply at the duct's boundaries but goes

down in the duct's center. In Figure4, we observed that the velocity distribution multiply with rise of Q whereas it go down by rise in m, as shown in Figure5. Fig 6 demonstrates the effect of k on u. It is seen that u goes down slowly at the duct's boundaries, however rise at the central part of the duct with rise k.

Figure7. Shown the effect of viscosity parameter α on u, at the left part of the duct the velocity go down by rising α and the opposite behavior noted for the right part of the duct. From figs. 8 and 9 noted that u do not change at rise in Br and Bn. Figure10 displayed the effect of ϕ_1 on the u.

When ϕ_1 is rises, the speed on the axis of the channel rise at the right wall and merges from the middle part to the remainder of the channel (no effect). Figure11 explained that the speed on the axis of flow rising near the left wall and center section of the duct, but the situation is reversed near the right side of the duct, by rising in ϕ_2.

Fig 12 we noted that at rising in φ, merges from the center part to the right wall of the duct and u go down at the left. There is a lot of agreement between our results for $M, \alpha, \phi_1, \phi_2$ and φ with those reported in Murad and Abdulhadi [18,19].
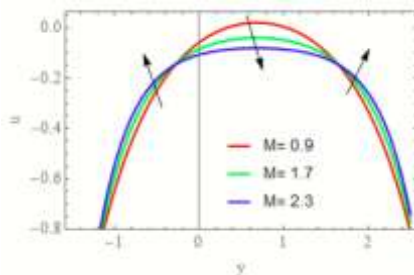
Fig. 2: The axial velocity u affect by M at$\phi_1 = 2, \phi_2 = 1, m = .1$, $Q = 1.3, k = 1, \alpha = 0.03, \beta = 0.2, \varphi = \frac{\pi}{4}, Br = 5, Bn = .001, x = .1$
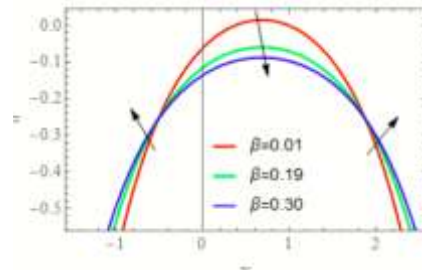
Fig. 3: The axial velocity u affect by β at$\phi_1 = 2, \phi_2 = 1, m = .1$, $Q = 1.3, k = 1, \alpha = 0.03, M = 0.9, \varphi = \frac{\pi}{4}, Br = 5, Bn = .001, x = .1$
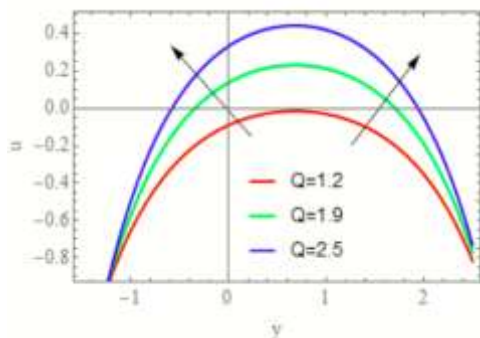
Fig. 4: The axial velocity u affect by Q at$\phi_1 = 2, \phi_2 = 1, m = .1,$
$Q\ k = 1, \alpha = 0.03, M = 0.9, \beta = 0.2, \varphi = \frac{\pi}{4}, Br = 5, Bn = .001, x = .1$
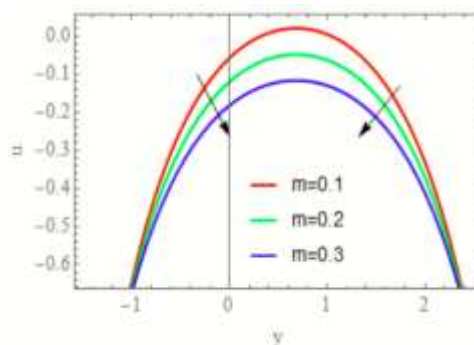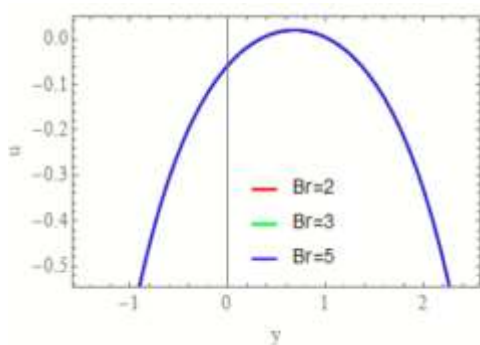

Fig. 5: The axial velocity u affect by m at$\phi_1 = 2, \phi_2 = 1, k = 1,$
$Q = 1.3, \alpha = 0.03,, M = 0.9, \beta = 0.2, \varphi = \frac{\pi}{4}, Br = 5, Bn = .001, x = .1$
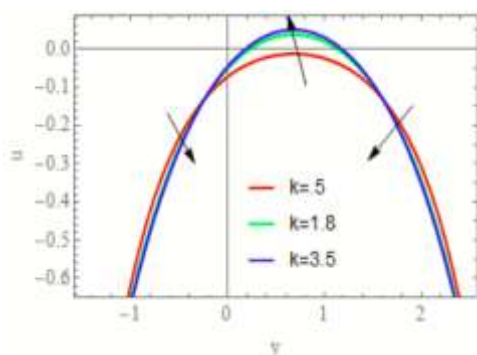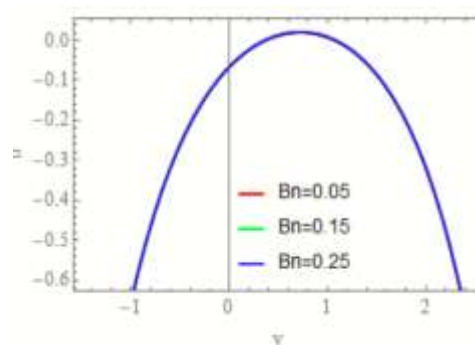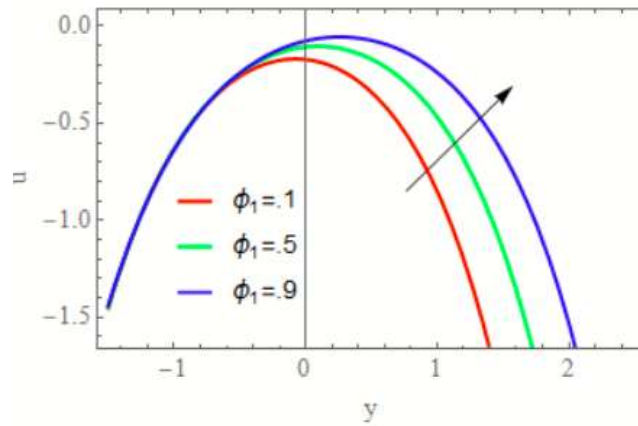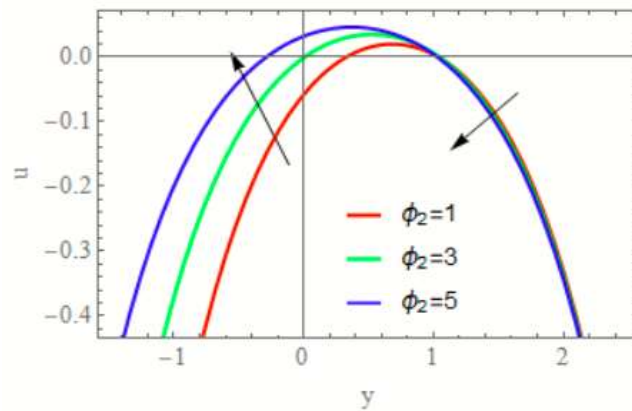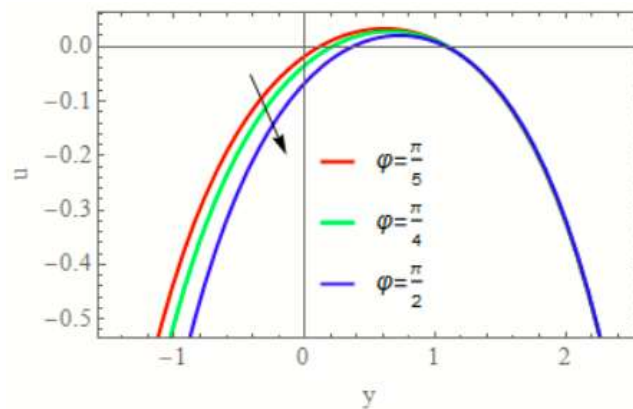

Fig. 6: The axial velocity u affect by k at$\phi_1 = 2, \phi_2 = 1, m = .1,$
$\alpha = 0.03, Q = 1.3, M = 0.9, \beta = 0.2, \varphi = \frac{\pi}{4}, Br = 5, Bn = .001, x = .1$
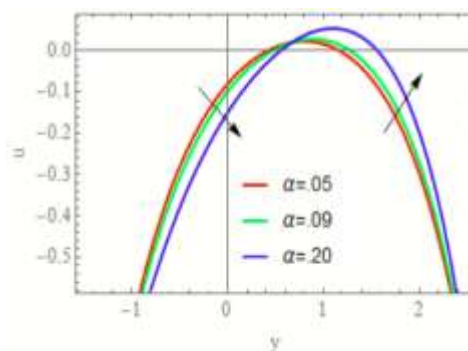
Fig. 7: The axial velocity u affect by α at$\phi_1 = 2, \phi_2 = 1, m = .1,$
$k = 1, Q = 1.3, M = 0.9, \beta = 0.2, \varphi = \frac{\pi}{.}, Br = 5, Bn = .001, x = .1$

Fig. 8: The axial velocity u affect by Br at$\phi_1 = 2, \phi_2 = 1, m = .1$
$k = 1, \alpha = 0.03, Q = 1.3, M = 0.9, \beta = 0.2, \varphi = \frac{\pi}{4}, Bn = .001, x = .1$

Fig. 9: The axial velocity u affect by Bn at$\phi_1 = 2, \phi_2 = 1, m = .1$
$k = 1, \alpha = 0.03, Q = 1.3, M = 0.9, \beta = 0.2, \varphi = \frac{\pi}{4}, Br = 5, x = .1$

Fig. 10: The axial velocity u affect by ϕ_1 at $\phi_2 = 1, m = .1, k = 1$
$k\ \alpha = 0.03, Q = 1.3\ , M = 0.9, \beta = 0.2, \varphi = \dfrac{\pi}{4}, Br = 5, Bn = .001, x = .1$

Fig. 11: The axial velocity u affect by ϕ_2 at $\phi_1 = 2\ , m = .1, k = 1$
$k\ \alpha = 0.03, Q = 1.3\ , M = 0.9, \beta = 0.2, \varphi = \dfrac{\pi}{4}, Br = 5, Bn = .001, x =$

Fig. 12: The axial velocity u affect by φ at $\phi_1 = 2\ , \phi_2 = 1, m = .1, k = 1$
$k\ \alpha = 0.03, Q = 1.3\ , M = 0.9, \beta = 0.2, , Br = 5, Bn = .001, x = .1$

Temperature distribution θ

The temperature profile variation for various values of the related parameters is depicted in the Figs. 13-23. Figure13 shown that the effect of M on the temperature profile, It is noticed that the temperature profile go down with rise M. Figs 14 and 15 explained the temperature distribution go down in the middle part and multiply at the boundaries of the duct by rise β and m, However, the converse is true when rising in Q and Br, as illustrate in shown in figs. 16 and 17. Fig 18 illustrate the influence of k on θ. It is noticed that when rise in k, the θ rising in the central region and the right wall of the duct and gradually vanishes from the left wall of the duct. In fig 19 we noted that by rising Gr, the temperature goes down in the center region, but rises in the right wall of the duct and gradually vanishes from the left wall of the duct. With rising in Bn ,the temperature distribution exhibits oscillatory behavior as in Figure20. The temperature distribution rises along the right wall, and then gradually disappear by rising in ϕ_1 as shown in Figure21. From fig 22 we noted that at rising in ϕ_2, the temperature rises at the duct 's left wall and blends with rest of the duct 's middle portion (no effected). From Figure23 we noticed that when φ rises, θ go down at the left wall of the duct and merges from the middle area to the duct 's right wall. The impacts of Br, Gr, k, ϕ_1, ϕ_2 and φ. Consistent with results analyzed in previous studies (Murad and Abdulhadi[18,19].
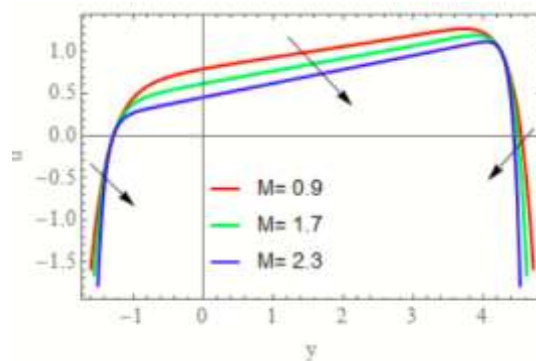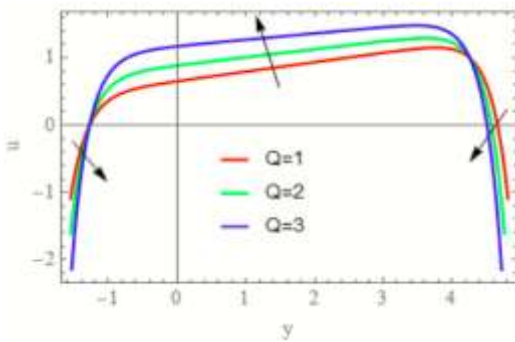

Fig. 13: The temperature profile θ affect by M at $\phi_1 = 4, \phi_2 = 3, m = .2$
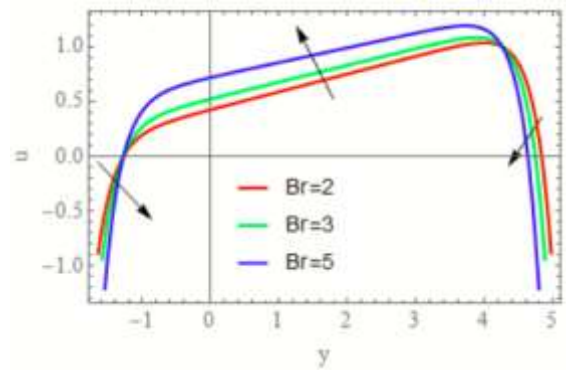$k = 3, Gr = .001, Q = 1.3 , \beta = 0.2, \varphi = \dfrac{\pi}{4}, Br = 5, Bn = .1, x = .1$
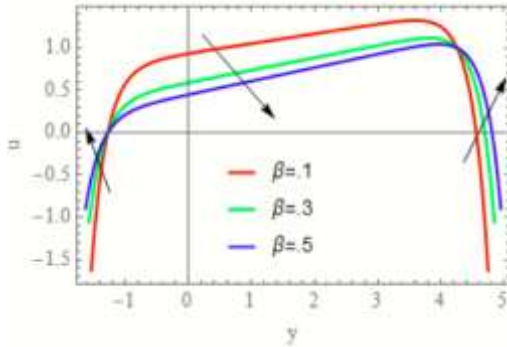
Fig. 14: The temperature profile θ affect by β at $\phi_1 = 4, \phi_2 = 3, m = .2$ $k = 3, Gr = .001, Q = 1.3, M = 2, \varphi = \frac{\pi}{4}, Br = 5, Bn = .1, x = .1$
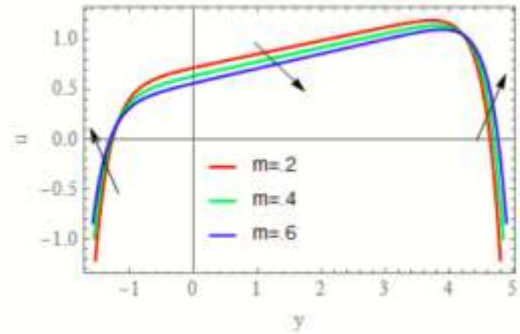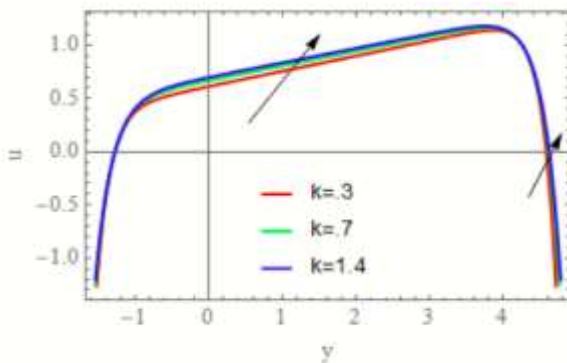

Fig. 15: The temperature profile θ affect by m at $\phi_1 = 4, \phi_2 = 3, k = 3$ $M = 2, Gr = .001, Q = 1.3, \beta = 0.2, \varphi = \frac{\pi}{4}, Br = 5, Bn = .1, x = .1$
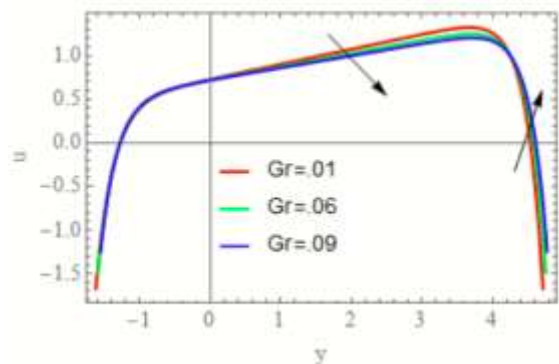

Fig. 16: The temperature profile θ affect by Q at $\phi_1 = 4, \phi_2 = 3, k = 3$ $M = 2, Gr = .001, m = .2, \beta = 0.2, \varphi = \frac{\pi}{4}, Br = 5, Bn = .1, x = .1$
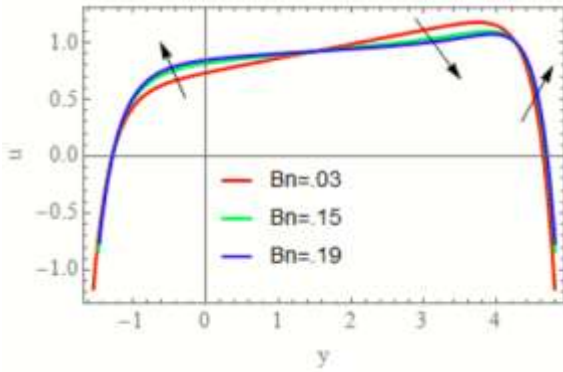

Fig. 17: The temperature profile θ affect by Br at $\phi_1 = 4, \phi_2 = 3, k = 3$ $M = 2, Gr = .001, Q = 1.3, \beta = 0.2, \varphi = \frac{\pi}{4}, m = .2, Bn = .1, x = .1$
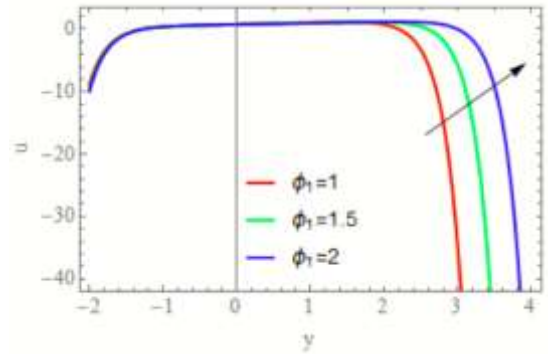

Fig. 18: The temperature profile θ affect by k at $\phi_1 = 4, \phi_2 = 3, m = .2$ $M = 2, Gr = .001, Q = 1.3, \beta = 0.2, \varphi = \frac{\pi}{4}, Br = 5, Bn = .1, x = .1$
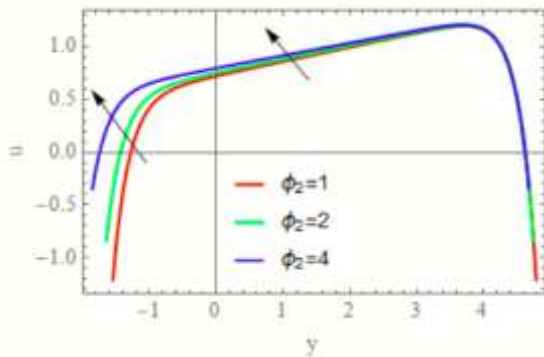

Fig. 19 : The temperature profile θ affect by Gr at $\phi_1 = 4, \phi_2 = 3, m = .2$ $M = 2, k = 3, Q = 1.3, \beta = 0.2, \varphi = \frac{\pi}{4}, Br = 5, Bn = .1, x = .1$
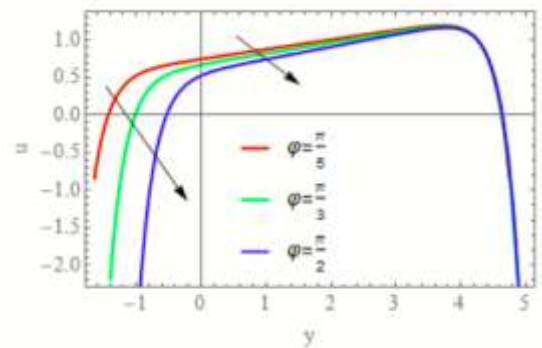
Fig. 20 : The temperature profile θ affect by Bn at $\phi_1 = 4, \phi_2 = 3, m = .2$
$M = 2, Gr = .001, Q = 1.3, \beta = 0.2, \varphi = \frac{\pi}{4}, Br = 5, k = 3, x = .1$

Fig. 21 : The temperature profile θ affect by ϕ_1 at $\phi_2 = 3, m = .2, M = 2,$
$Gr = .001, Q = 1.3, \beta = 0.2, \varphi = \frac{\pi}{4}, Bn = .1, Br = 5, k = 3, x = .1$

Fig. 22 : The temperature profile θ affect by ϕ_2 at $\phi_1 = 4, m = .2, M = 2,$
$Gr = .001, Q = 1.3, \beta = 0.2, \varphi = \frac{\pi}{4}, Bn = .1, Br = 5, k = 3, x = .1$

Fig. 23 : The temperature profile θ affect by φ at $\phi_1 = 4, m = .2, M = 2,$
$Gr = .001, Q = 1.3, \beta = 0.2, \phi_2 =, Bn = .1, Br = 5, k = 3, x = .1$

Conclusions

In this study, the effect of heat transfer and slip condition on peristaltic transport of MHD non-Newtonian fluid across tapered porous channel at low Reynolds number and a long wavelength are utilized. The perturbation method was used to solve a system of nonlinear partial differential equations of this research. The following are some of the more intriguing analyses:

❖ When M and β is rised, the velocity on the axis of flow go down in the central region and grows near the duct 's edges, but the opposite occur for rise k. By rising Q,the velocity multiply across the entire cross-section, but go down with rising m.

❖ Velocity on the axis of flow while it grows on the right side of the channel, go down near the left by rises α. Also, the velocity is unaffected by Br andBn.

❖ The θ go down by rise M. It's go down in the central region and grows near the duct 's edges by rise m and β, but the opposite occur for rise Q and Br.

❖ By rising Gr, the temperature go down in the center region, but growth in right wall of the duct and gradually vanishes from the left wall of the duct.

References

1. M. G. Rabby, A. Razzak, M. M. Molla, Procedia Engineering, 56(5),225-231(2013)
2. E. Falk, K. S. Prediman, V. Fuster, Coronary plaque disruption Circulation, 92(3), 657-671(1995)
3. J. C. Burns, T. Parkes, Journal of Fluid Mechanics, 29, 731-743(1967)
4. M. Y. Jaffrin, A. H. Shapiro, S. L. Weinberg, Journal of Fluid Mechanics, 37, 799–825(1969)
5. H. S. Lew, Y. C. Fung, C. B. Lowenstein, Journal of Biomechanics, 4, 297–315(1971)
6. E. F. Elshehawey, Z. M. Gharsseldien, Appl. Math. Computation, 153, 417–432(2004)
7. A. Abd El Naby, A. E. M. El Misery, I. I. El Shamy, Applied Mathematics and Computation, 58(2), 497-511(2004)
8. T. Hayat, N. Ali, Appl. Math. Modell, 32, 761-774(2008)
9. S. Nadeem, T. Hayat, N. S. Akbar, M.Y. Malik, Int. J. Heat Mass Transfer, 52, 4722-4730(2009)
10. S. Farooq, M. Awais, M. Naseem, T. Hayat, B. Ahmad, Nuclear Engineering and Technology, 49, 1396-1404(2017)
11. B. Tripathi, B. K. Sharma, Int. J. of Applied Mechanics and Engineering, 23(3), 767-785(2018)
12. A. B. Huda, N. Sh. Akbar, O. A. Beg, M. Y. Khan, Results in Physics, 7, 413–425(2017)
13. N. Ali, K. Ullah, H. Rasool, Physics of Fluid 32, 073104(2020)
14. S. S. Hasen, A. M. Abdualhadi, Iraq Journal of Science, 61(6), 1461-1472(2020)
15. R. S. Kareem, Abdualhadi, Iraqi Journal of Science, 61(4), 854-869(2020)
16. J.C. Misra, B. Mallick, A. Sinha, Alexandria Engineering Journal, 57,391-406(2018)
17. M. R. Salman, A. M. Abdulhadi, International Journal of Science and Research, 7(2), 612-623(2018)
18. M. A. Murad, A. M. Abdulhadi, Journal of Al-Qadisiyah for Computer Science and Mathematics, 12(4), 79-90(2020)
19. M. A. Murad, A.M. Abdulhadi, Journal of Physics: Conference Series, 1804 012060(2021)
20. T. Hayat, S. Noreen, M. Shabab Alhothuali, S. Asghar, A. Alhomaidan, International Journal of Heat and Mass Transfer, 55, 443-452(2012)
21. M. A. Murad, M. Ahmed, Flow Analysis of non-Newtonian, Herschel-Bulkily Fluids and Some of Its Special Cases .Thesis submitted to college of since-university of Baghdad, Baghdad-Iraq,(2021)